PAPER

Circularly Polarized Printed Antenna Combining Slots and Patch

Toshimitsu TANAKA[†a)], **Tamotsu HOUZEN**[†], ***Student Members***, **Masaharu TAKAHASHI**[††], ***and*** **Koichi ITO**[†††], ***Members***

SUMMARY In this paper, the authors propose a circularly polarized printed antenna combining a slot array antenna and a patch antenna, with dual-band operation. The proposed antenna has good isolation performance, is compact, and has simple configuration. This antenna is composed of two parts, a patch antenna (for Rx) on the top, and a slot array antenna (for Tx) on the bottom, respectively. The element layout is such that the lower radiation element is not hidden by the upper one for wide observation angle. Hence, both radiation elements can naturally radiate the targeted polarization. Both slot array and patch antenna are fed by electromagnetically coupled microstrip line feed. With such a configuration, it is possible to efficiently obtain good isolation characteristics for both frequency bands. Furthermore, this antenna can be easily composed and it is not necessary to use any feeding pin or via hole. The target of this antenna is mobile communications applications such as mobile satellite communications, base-station of wireless LAN, etc. Here, the design techniques are discussed and the numerical and experimental analyses are presented.
key words: *dual-band, patch antenna, slot antenna, circular polarization, electromagnetically coupled microstrip line feed*

1. Introduction

In recent years, the rapid growth of the mobile communications, for example mobile satellite communications, wireless LAN, etc., yields to many requirements for the antenna such as circularly polarized (CP) radiation, dual-band operation, good isolation characteristics, electromagnetically coupled feeding, small size and low-cost, etc. [1], [2].

Table 1 shows one example of specifications for the mobile satellite communications. This specification is based on the communication experiments by use of the Engineering Test Satellite VIII (ETS-VIII) [3] which will be launched by the Japan Aerospace Exploration Agency (JAXA) in FY 2006. From this table, the characteristic requirements are a left handed circular polarization (LHCP) for transmission (Tx) and reception (Rx) and a narrow frequency separation between Rx and Tx (5.8%). Patch antennas are a good candidate to meet such requirements, due to their various advantages. However, to meet all of these requirements as explained above is still a difficult problem.

Manuscript received June 20, 2006.
Manuscript revised September 25, 2006.
[†]The authors are with the Graduate School of Science and Technology, Chiba University, Chiba-shi, 263-8522 Japan.
[††]The author is with the Research Center for Frontier Medical Engineering, Chiba University, Chiba-shi, 263-8522 Japan.
[†††]The author is with the Department of Medical System Engineering, Chiba University, Chiba-shi, 263-8522 Japan.
a) E-mail: toshi.tanaka@m.ieice.org
DOI: 10.1093/ietcom/e90–b.3.621

Table 1 Target of the antenna for mobile satellite communications.

Frequency bands	Reception (Rx) (patch antenna)	2.50 GHz Bandwidth:25 MHz
	Transmission (Tx) (slot antenna)	2.65 GHz Bandwidth:25 MHz
Polarization	Left-handed circular polarization (LHCP) for both Tx and Rx	
Minimum gain	more than 5 dBic at boresight	
Maximum axial ratio	less than 3 dB (in the on-axis direction)	
Isolation	more than 20 dBic	

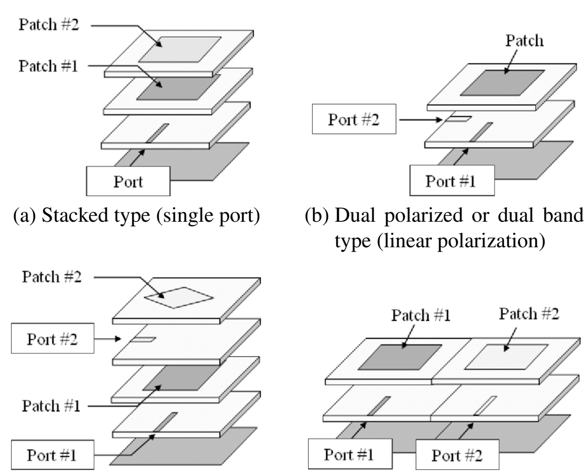

(a) Stacked type (single port) (b) Dual polarized or dual band type (linear polarization)
(c) Staked type (d) Coplanar type

Fig. 1 Reported dual-band or dual polarized patch antennas.

The typical types of reported dual-band or dual polarized antennas fed by electromagnetically coupling are shown in Fig. 1 and features are summarized in Table 2. The stacked type patch antenna [4]–[6] which is shown in Fig. 1(a) can operate at dual or wide-band. However, this kind of antennas has only a single input/output port. Thus, in case of mobile satellite communications, a high performance diplexer is necessary to split the Tx and Rx signals because the frequency separation between them is narrow and the difference of signal level is more than 100 dB. Therefore, to simplify the system, the antenna would better have dual ports (Tx port and Rx port) with good isolation performances.

Figures 1(b) and (c) shows the dual-band or dual-polarized antenna. Although these types of antenna can have good isolation characteristics between the two ports, the polarization is linear only and each port should be orthogonally placed because both a use of separate feed points located along the perpendicular center lines of the antenna and an excitation of the orthogonal modes (TM_{10}, TM_{01}) are necessary to increase the isolation characteristics [7].

Figure 1(c) [8] has some possibilities to obtain dual-band circular polarization and isolation characteristics. However, optimization of the resonant frequency and generation of the CP radiation is difficult owing to the high mutual coupling between the upper and the lower patch while CP is generated. Therefore, a lot of design time and many shorting pins are necessary. Although Fig. 1(d) has also the same possibilities, a wide space compared with the stacked configuration is necessary. Moreover, difficulty in obtaining good axial ratio characteristics is considered due to the asymmetrical ground plane. With self-diplexing antennas [9], CP radiation, dual-band operation and isolation performances can be obtained. However, many shorting pins and complex feeding constructions are necessary. Moreover, in this composition, it is very difficult to apply an electromagnetic coupling feed. From an industrial point of view, a more simple and low-cost structure such as stacked configuration and electromagnetically coupled feed are required.

In this paper, a circularly polarized printed antenna combining slots and patch is presented. With the proposed configuration a dual-band operation, good isolation characteristics and generation of a circular polarization for both frequencies can be obtained. Moreover, an electromagnetic coupling feed as required for mobile communications use can be employed.

This antenna is composed of two parts which are a patch antenna (for Rx) on the top, and a slot array antenna (for Tx) on the bottom. With this unique novel configuration, both antennas can radiate a circular polarization and it efficiently allows good isolation characteristics. Moreover, an electromagnetically coupled microstrip feeding is used for all the elements. Consequently, this antenna can simply be constructed by use of multilayer printed circuit boards, and the soldering process for feeding pin or via hole is eliminated.

Section 2 of this paper presents the construction and the design parameter of the slot array and the patch antenna. Section 3 describes the numerical analysis by use of the Method of Moments (MoM) and the experimental result. Finally, this study is summarized and concluded in Sect. 4.

Table 2 Features of the reported dual-band or dual polarized printed antennas.

Type	Number of Port	Polari -zation	Isolation	Area	Thickness
(a) [4], [5] [6], [7]	1	LP:○ CP:○	×	small	thin
(b) [7]	2	LP:○ CP:×	○	small	thin
(c) [8]	2	LP:○ CP:×	○	small	thin
(d)	2	LP:○ CP:△	○	wide	thin
Proposed antenna	2	LP:○ CP:○	○	small	thick★

○:easy, △:relatively difficult, ×:difficult
★: in case of using a reflector for the slot layer

2. Antenna Configuration and Design

Figure 2 shows the geometry of the circularly polarized printed antenna combining slots and patch. A CP patch antenna is located on the upper side, while a CP slot array antenna, which is placed around the patch antenna is etched on the ground plane. One advantage of this element layout is that the lower radiating element is not hidden by the upper one for wide observation angle. Hence, the slot array antenna on the lower layer can naturally radiate the targeted polarization. In case of usual stacked type patch antennas (see Fig. 1(c)), the lower element is hidden by the upper patch element for wide angle and the mutual coupling is high.

Feeding lines for the microstrip antenna and the slot array are located on both sides of the ground plane, hence the mutual coupling between two microstrip feeding lines is reduced.

The operation frequency is set to 2.50 GHz for the patch antenna which is connected to port 1 and 2.65 GHz for the slot array antenna which is connected to port 2. The frequency separation between port 1 and port 2 is 5.8% and the polarization is a left-handed circularly polarization (LHCP) for both frequencies.

2.1 Patch Antenna Layer

Figure 3 shows the geometry of the circularly polarized patch antenna layer. The substrate structure consists of layer-I and layer-II made of fiberglass/PTFE composite materials (ϵ_r = 2.17) and each thickness is 0.8 mm. The radiation element on the layer-I is a square microstrip with square

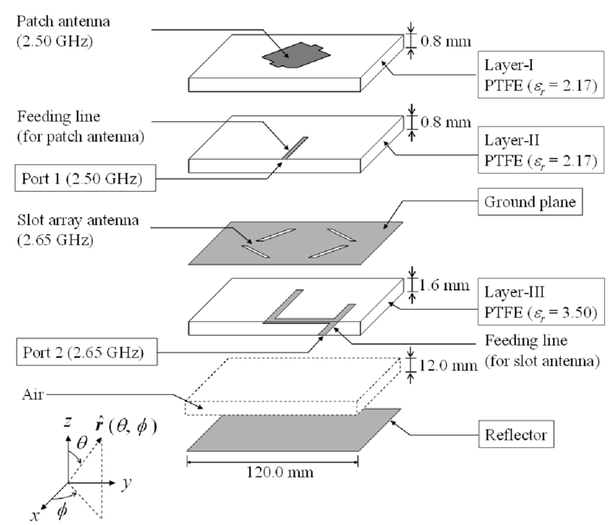

Fig. 2 Geometry of the circularly polarized printed antenna combining slots and patch.

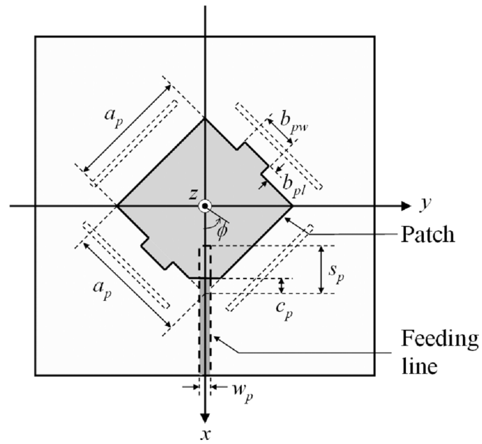

Fig. 3 Geometry of the circularly polarized patch antenna layer. a_p = 38.8, b_{pw} = 6.1, b_{pl} = 1.9, c_p = 2.0, s_p = 17.5, w_p = 2.3 [mm].

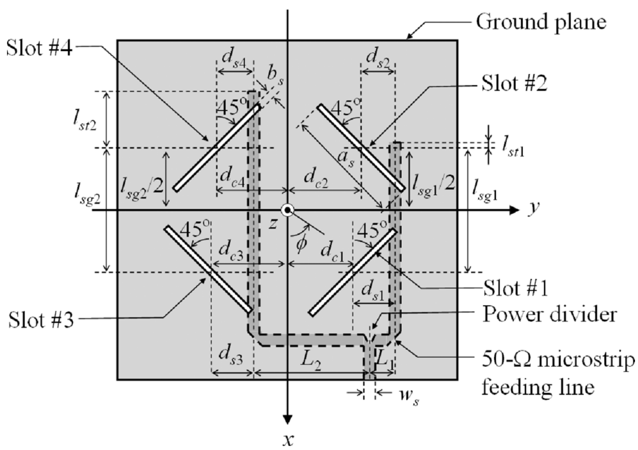

Fig. 4 Geometry of the 4-element circularly polarized slot array antenna layer. a_s = 37.8, b_s = 1.0, d_{s1} = 13.5, d_{s2} = 12.5, d_{s3} = 13.5, d_{s4} = 12.5, d_{c1} = 21.0, d_{c2} = 22.0, d_{c3} = 22.0, d_{c4} = 21.0, l_{sg1} = 34.4, l_{sg2} = 34.4, l_{st1} = 7.8, l_{st2} = 25.3, L_1 = 4.3, L_2 = 38.7, w_s = 3.6 [mm].

perturbation segments; ($2 \cdot b_{pl} \cdot b_{pw}$) to generate a CP radiation by a single point feeding [10]. The feeding method is the electromagnetic coupling (proximity coupling) by use of a 50-Ω microstrip line placed on layer-II [11]. Moreover, in order to obtain a good impedance matching, the corner of the microstrip element, which length is c_p, is cut.

2.2 Slot Array Antenna Layer

Figure 4 shows the geometry of the 4-element circularly polarized slot array antenna layer. All slot elements are etched on the ground plane of the patch antenna. This ground plane is placed between layer-II and layer-III. Layer-III consists of Fiber-glass/PTFE composite materials (ϵ_r = 3.5) and is used to support the slots and their feeding network. This choice of material decreases the length of the slots and keeps a fairly low loss of microstrip line. Furthermore, in order to realize the stacked configuration and low-cost performances, the electromagnetic coupling feed by use of a 50-Ω microstrip line is used. The width and length of the slots are b_s and a_s, respectively. At the bottom of this antenna, a reflector is mounted to reduce the back radiation. Although this reflector makes the antenna thick, a low profile cavity slot configuration [12] will be applied and thin configuration is available.

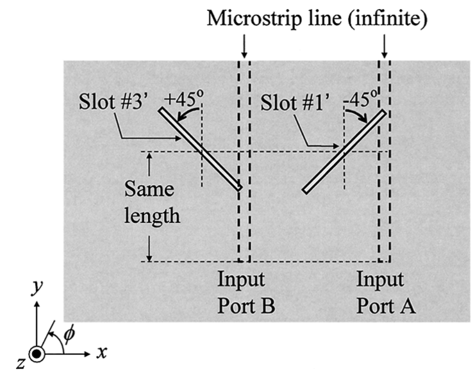

Fig. 5 Calculation model for estimation of phase difference.

This slot array consists of two slots pairs, namely slot #1-#2 and slot #3-#4. All slots are ±45° inclined compared to the microstrip feed line direction, in other words, slot #1 and #2 (or slot #3 and #4) are orthogonal, and slot #1 and slot #4 (or slot #2 and slot #3) are parallel to each others.

The design procedure of slots pair (slot #1 and #2) is as follows. The slot #2 is designed to be a matching element [13] of the microstrip transmission line. The position of slot #2 is determined in terms of length of open stub l_{st1} that is as short as possible. The element spacing l_{sg1} is designed to radiate LHCP by referencing the radiated electric field from slot #2. For realizing a uniform distribution, resistance value of slot #1 is controlled by the offset value d_{s1}. Employing the same technique, the other slot pair (slot #3 and #4) is designed.

To realize a single input port and a compact design, a power divider [14] and correction of the phase difference between two slots pairs by use of microstrip line are necessary. Figure 5 shows the calculation model to estimate the phase of electric field radiated by slot #1 and slot #3 by using MoM. Although infinite length of microstrip lines are used for this model, other parameter (materials, stack configuration, slot length, element spacing, offset length) are the same as Fig. 4. From this calculation, the phase difference between two slots are almost $1/2\ \pi$ (87°). This phase difference induces RHCP radiation. Therefore, the difference of microstrip line length between L_1 and L_2 is set to $1/2\ \lambda_g$ to generate LHCP radiation.

With reference to time-phase difference and direction of the magnetic current of Fig. 6, the relative phase difference for LHCP radiation can be easily understood. As shown in this figure, slot #1 and slot #4 are in co-phase, slot #2 and slot #3 are also in co-phase. The relative phase difference between slot #1 and slot #2 is $\pi/2$. Additionally, all slot elements have the same amplitude.

The radiation characteristics of this slot array, especially the axial ratio characteristics, are easily estimated us-

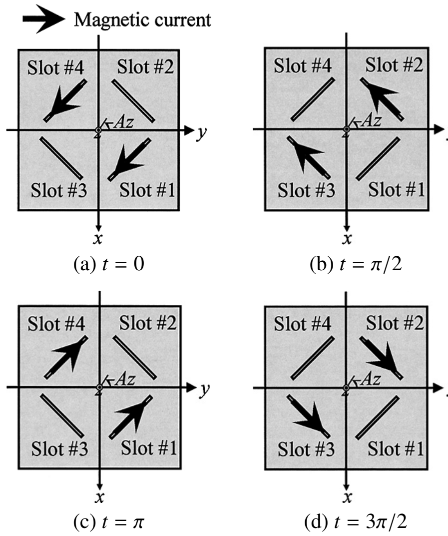

(a) $t = 0$ (b) $t = \pi/2$

(c) $t = \pi$ (d) $t = 3\pi/2$

Fig. 6 Time-phase of the magnetic current on the 4-element circularly polarized slot array antenna (in case of LHCP).

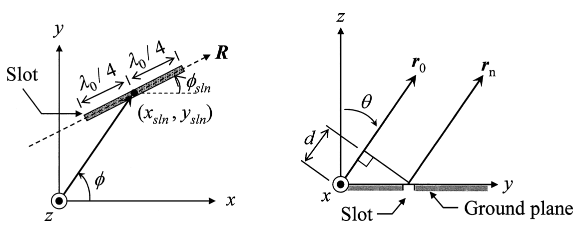

(a) Arbitrary rotated slot on the xy plane (b) Far-field observations

Fig. 7 Geometry of an arbitrary rotated slot.

ing the following line source model.

Consider an arbitrary slot on an infinite ground plane (xy-plane) as shown in Fig. 7. The coordinate point of the center of the slot #n is (x_{sln}, y_{sln}) and the inclined angle from the x-axis is ϕ_{sln}. The slot length a_s is 1/2 λ_0 (half wavelength) and the magnetic current distributions on the slots are assumed to be a sinusoidal curve.

The arbitrary point and the magnetic current on the nth slot are respectively expressed as

$$(x, y) = (x_{sln} + R\cos\phi_{sln}, y_{sln} + R\sin\phi_{sln}) \quad (1)$$

$$M(R) = M_0 \cos(k_0 R) \quad (2)$$

where, $M(R)$ is the magnetic current distribution, R is the axis along the slot and the range is

$$-\lambda_0/4 \le R \le \lambda_0/4 \quad (3)$$

Then, the electric field E_{sln} at (θ, ϕ) radiated by a single slot is expressed as

$$\boldsymbol{E}_{sln} = \int_{-\lambda_0/4}^{\lambda_0/4} jk_0 \frac{M_0}{4\pi} \frac{e^{-jk_0(r-d)}}{r-d} \cos(k_0 R) \{\hat{\boldsymbol{\theta}} \sin(\phi - \phi_{sln}) + \hat{\boldsymbol{\theta}} \cos\theta \cos(\phi - \phi_{sln})\} dR$$

$$= jk_0 \frac{M_0}{2\pi} \frac{e^{-jk_0 r}}{r} (\cos A_{sln} + j \sin A_{sln}) \frac{\cos(\frac{\pi}{2} B_{sln})}{1 - B_{sln}}$$

$$(\hat{\boldsymbol{\theta}} \sin(\phi - \phi_{sln}) + \hat{\boldsymbol{\phi}} \cos\theta \cos(\phi - \phi_{sln})) \quad (4)$$

where,

$$d = \{(x_{sln} + R\cos\phi_{sln})\cos\phi + (y_{sln} + R\sin\phi_{sln})\sin\phi\}\sin\theta \quad (5)$$

$$A_{sln} = k_0 (x_{sln}\cos\phi + y_{sln}\sin\phi)\sin\theta$$

$$B_{sln} = (\cos\phi_{sln}\cos\phi + \sin\phi_{sln}\sin\phi)\sin\theta \quad (6)$$

In order to calculate each radiated electric fields E_{sl1} to E_{sl4}, substitute each slot parameters in equations (4). Then, the total radiation electric field E_{sl} radiated by a 4-element slot array, assuming no coupling between the elements, can be described as,

$$\boldsymbol{E}_{sl} = \boldsymbol{E}_{sl1} + e^{j\frac{\pi}{2}} \boldsymbol{E}_{sl2} + e^{j\frac{\pi}{2}} \boldsymbol{E}_{sl3} + \boldsymbol{E}_{sl4} \quad (7)$$

The axial ratio is calculated from

$$AR_{sl} = \frac{|\boldsymbol{E}_{Rsl}| + |\boldsymbol{E}_{Lsl}|}{|\boldsymbol{E}_{Rsl}| - |\boldsymbol{E}_{Lsl}|} \quad (8)$$

where,

$$|\boldsymbol{E}_{Rsl}| = \frac{1}{\sqrt{2}} |\boldsymbol{E}_{\theta sl} + j\boldsymbol{E}_{\phi sl}|$$

$$|\boldsymbol{E}_{Lsl}| = \frac{1}{\sqrt{2}} |\boldsymbol{E}_{\theta sl} - j\boldsymbol{E}_{\phi sl}| \quad (9)$$

Although, in this formula, the length of the slot is set to 1/2 λ_g to simplify the formula, the actual slot length is slightly shorter because these slots are non-resonant and covered by a dielectric substrate. By use of this equation, the radiation of a circularly polarized wave is confirmed and the ideal 3-dB axial ratio beamwidth is 88°. Figure 8 shows the external view and the top view of the fabricated antenna. The ground plane size is 120 mm × 120 mm for measurement.

2.3 Influence of the Patch Element and the Dielectric Layer

The slot antenna is covered by the patch layer whose height, relative permittivity and dielectric loss tangent are 1.6 mm, 2.17, and 0.0009, respectively. Thus, it is considered that the radiation characteristics of the slot array are influenced by the patch element and the dielectric layer. Figure 9 shows the comparison of the radiation characteristics between the slot antenna with a patch antenna layer and the slot antenna only in the xz-plane. These results were obtained by numerical simulation by use of the Method of Moments. In order to investigate the influence of the patch antenna and its dielectric layer above the slot, two straightforward microstrip lines are used to independently feed the two-slot pairs. Thus, the influence of the power divider, bend of the microstrip line are not included in Fig. 9.

From this figure, although the maximum gain decreases of 0.5 dB because of the dielectric layer, the axial ratio characteristics and radiation pattern are almost the same in both

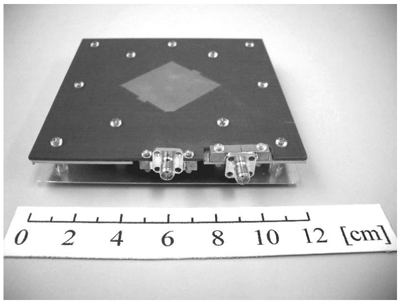

(a) External view

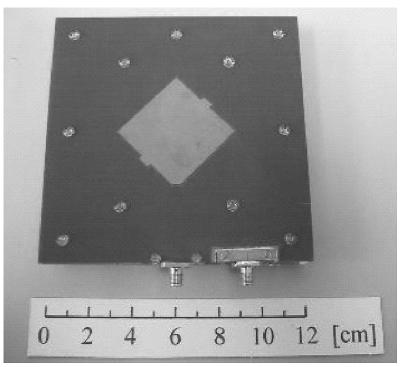

(b) Top view of the patch antenna layer (layer I)

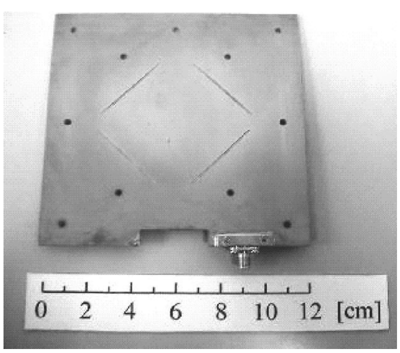

(c) Top view of the slot antenna layer (ground plane)

Fig. 8 Fabricated antenna.

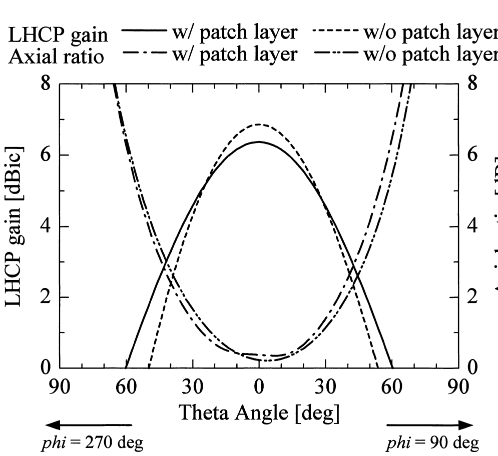

Fig. 9 Comparison of the radiation characteristics between slot antenna with patch layer and without patch layer.

cases. Thus, it can be said that the patch antenna placed on the slot antenna does not influence the radiation characteristics of the slot array antenna.

Since mutual coupling between slot and patch is fairly week, influence of stacked configuration on the input impedance is low. Therefore, this slot array antenna can obtain the CP radiation without radiation conductor of the patch antenna, and each element can be designed separately. The patch antenna can also design and obtain the CP radiation without slot element. It can be said that the stacked configuration has practically less effect on the tendency of input impedance. Of course, since a few frequency shifting will be occurred when patch antenna (or slot antenna) is stacked, the adjustment of operating frequency is necessary.

3. Design Example and Results

This time, assuming that the antenna will be used for the mobile satellite communications, the specification and design target are shown in decided Table 1. This specification is based on the mobile satellite communication experiments as explained Sect. 1.

The patch antenna layer was designed for reception (2.50 GHz) and the slot antenna layer was designed for transmission (2.65 GHz), namely, port 1 is for reception, port 2 is for transmission. Each part was numerically optimized by minimizing the axial ratio in the boresight direction. It should be noted that the outline of the design procedure is almost same as the reported proximity coupled patch antenna and printed slot antenna [10], [11], [15].

The Method of Moments (MoM) has been chosen in the numerical analysis for its asset of fast calculation. Owing to the software characteristics, the dielectric substrate and the ground plane are considered to be infinite. The performances are compared with measurements realized in a radio anechoic chamber. In this section, numerical simulation and experimental results of the proposed antenna are shown.

3.1 Frequency Characteristics

Figure 10(a) and (b) show the relationship between the 3 dB-axial ratio bandwidth at boresight and the frequency. The minimum axial ratio of the patch antenna (Rx) obtained is 0.5 dB at 2.498 GHz by simulation, and 0.7 dB at 2.558 GHz by measurement. The minimum axial ratio of the slot antenna (Tx) is 0.4 dB at 2.647 GHz by simulation, and 0.2 dB at 2.758 GHz by measurement. These results show that this proposed antenna can radiate a CP and that good axial ratios can be obtained at both Rx and Tx bands.

The 3 dB-axial ratio bandwidths are 0.6% for the patch antenna (Rx) and 1.9% for the slot antenna (Tx) by simulation, 0.7% and 1.9% by measurement. A good agreement between measurement and simulation is observed. These data show the frequency characteristics of the patch antenna and the slot antenna are almost the same as the characteristics of the reported normal CP patch antenna [10], [16].

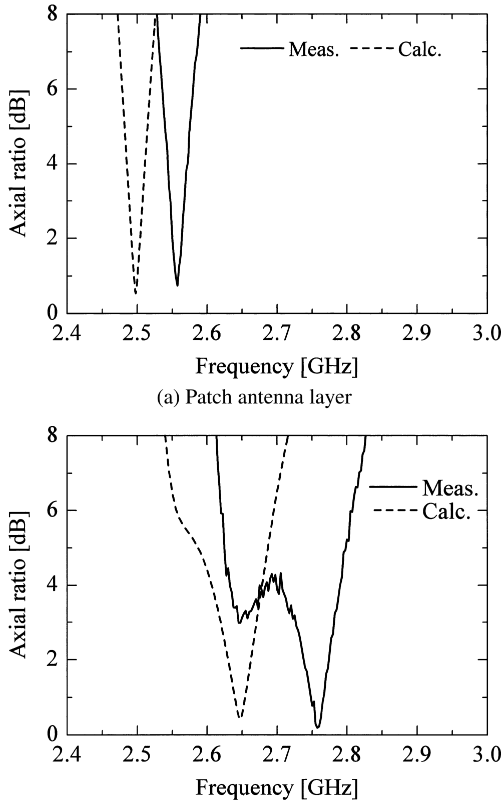

(a) Patch antenna layer

(b) Slot antenna layer

Fig. 10 Frequency characteristics of axial ratio.

Moreover, if necessary, it is considered that the reported bandwidth enhancement technique, such as using a parasitic element, can be used.

Although measurement and simulation results present the same tendency, the measurement results shows the minimum axial ratios of antenna are shifted to higher frequencies by 2.4% and 4.1% compared to the simulation results. The main reason is considered to be due to the effect of the ground plane size and difference of the feeding model. Especially, this difference of models induces a slight difference in the input impedance of the slot. Hence, it is considered that the frequency characteristics of the amplitude and phase of the slots were slightly shifted.

Figure 11 shows the relationship between the S-parameters for the simulated model and the measurement. S_{11} of the patch antenna layer (port 1) is shown in Fig. 11(a). The simulation and measurement results of the S_{11} are −23.6 dB and −15.7 dB, respectively.

Figure 11(b) shows the S_{22} of the slot antenna layer (port 2). The simulation result of the S_{22} is less than −13.4 dB over the 3-dB axial ratio bandwidth. However, the measurement result of the maximum S_{22} is −6.1 dB due to the 3-dB axial ratio bandwidth that is shifted to higher frequencies compared to the matched impedance bandwidth. As previously said, this shifting is explained by the influence of the ground plane size which is finite in the case of measurement while it is infinite by numerical simulation [17], [18]. Furthermore, the other error factors are the measurement systems and fabrication errors (i.e. space between each layer, cable, connectors, plastic screws, etc.) that affect the characteristics of the antenna. However, the measurement and simulation results present the same tendency.

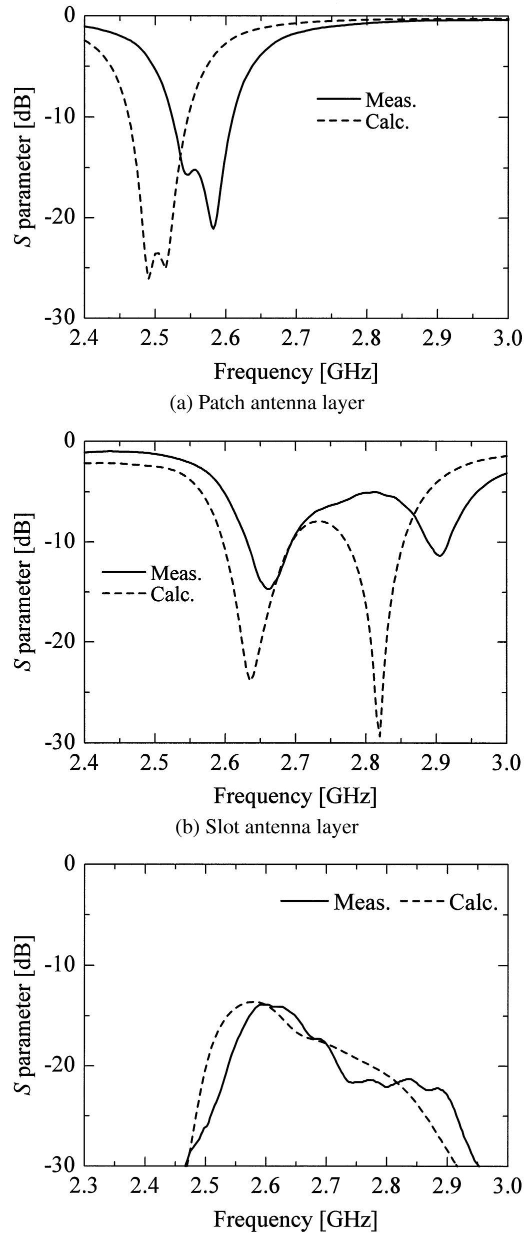

(a) Patch antenna layer

(b) Slot antenna layer

(c) Mutual coupling between patch and slots

Fig. 11 Frequency characteristics of S-parameter.

Figure 11(c) shows the isolation characteristics between patch (port 1) and slot (port 2). An isolation of more than 15 dB over the 3-dB axial ratio bandwidth for patch (Rx) and slot (Tx) has been achieved. Although the target is not satisfied, it can be said that the proposed stacked configuration has promising isolation characteristics and enables a CP radiation.

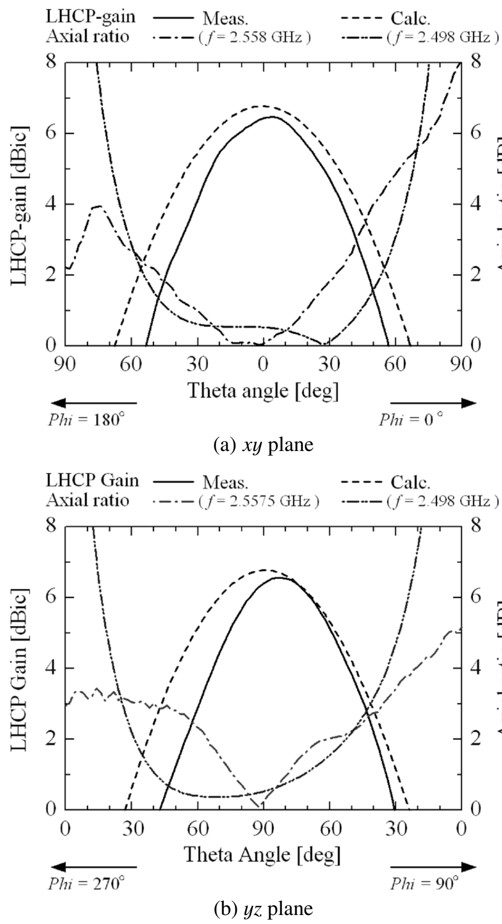

Fig. 12 Radiation characteristics of patch antenna.

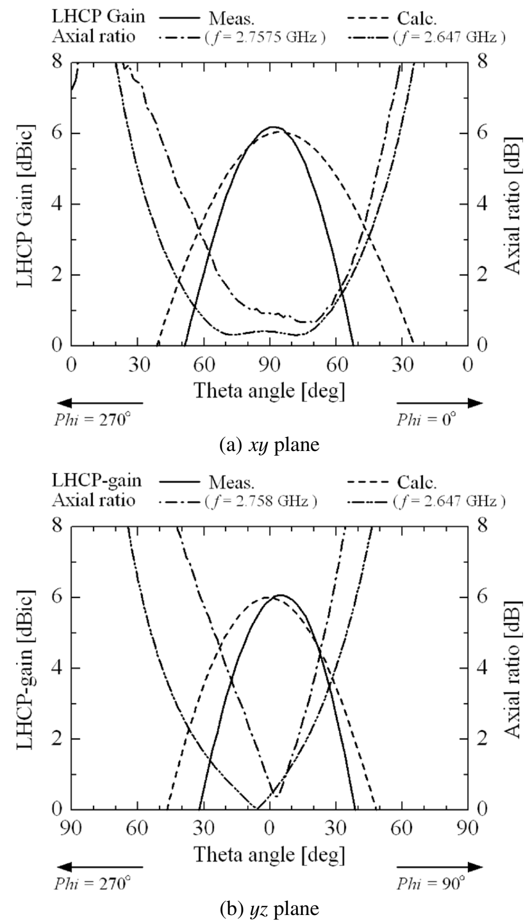

Fig. 13 Radiation characteristics of slot antenna.

3.2 Radiation Characteristics

Figures 12 and 13 represent the LHCP-gain and axial ratio characteristics. The full line and short dashed line represent the LHCP-gain characteristics obtained by numerical simulation and measurement, respectively.

Figures 12(a) and (b) show the radiation characteristics of the patch antenna (Rx) in the *xz* plane and *yz* plane. Although the measured axial ratio characteristics show a little asymmetry due to the two SMA connector and the ground plane diffraction, good circularly polarized patterns are obtained even with the slot antenna in the ground plane. The maximum radiation occurs when $\theta = 0°$ for the numerical simulation, $\theta = 8°$ of *yz* plane for the measurement. LHCP-gain and axial ratio for the boresight direction are 6.8 dBic and 0.5 dB by simulation, 6.4 dB and 0.1 dB by measurement respectively.

The minimum value of 3-dB axial ratio beamwidth is 112° in *yz* plane by simulation and 104° in *yz* plane by measurement. From these data, a CP radiation at boresight angle is confirmed and the radiation pattern is almost the same as the characteristics of reported normal patch antennas. In other words, the influence of the slot antenna under the patch element is low.

Figures 13(a) and (b) shows the radiation characteristics of the slot antenna (Tx) in the *xz* plane and *yz* plane. The maximum radiation occurs when $\theta = 0°$ by the numerical simulation, $\theta = 2°$ (in *xz* plane) by the measurement.

The simulated LHCP-gain and the axial ratio in the boresight direction are 6.0 dBic and 0.9 dB. Measured results are 6.2 dBic and 0.4 dB. Due to the beam narrowing, the measured gain is higher than calculated one. This beam narrowing is owed to the influence of the finiteness of the ground plane and its resulting diffraction [19], [20] as explained in the previous section. From Figs. 13(a) and (b), the axial ratio patterns are different between *xz* plane and *yz* plane due to the asymmetry configuration. However, good LHCP radiation is confirmed for boresight direction. The minimum value of 3-dB axial ratio beamwidth is 62° by simulation, 32° by measurement in *yz* plane. The half power beamwidth of that slot antenna are 64° by simulation, 48° in *yz* plane in measurement.

The measurement results of the patch antenna are shown to be in good agreement with the calculated ones compared with the slot antenna which are not. It can be explained that as the ground plane is a radiation conductor of the slot antenna, the size and shape are more effective than for the patch antenna. It should be noted that a good agreement of the measured and the calculated result of the finite ground plane model by use of FEM (HFSS ver.10) can be obtained. It can be supposed that a wide ground plane or attaching an absorbing material along the edge of ground plane is effective to reduce the diffraction.

From these results, a good CP radiation is confirmed and a LHCP gain more than 5 dBic and an axial ratio less than 3 dB are obtained. These results satisfy the target value for mobile satellite communications.

4. Conclusions

A circularly polarized printed antenna combining slots and patch in a stacked configuration has been proposed in this paper. The antenna can have a dual-band operation, good isolation characteristics and enables the generation of a circular polarization for both reception and transmission frequencies. The measurement results of the slot layer and the patch layer show the LHCP-gain and axial ratio in the boresight direction is more than 6 dBic and less than 1 dB, respectively. Moreover the isolation is more than 15 dB. In this paper, although the target polarization of this antenna was LHCP, another polarization can be obtained by changing the perturbations for the patch antenna and the phase distributions of the slot antenna array.

In the future, for the reduction of the thickness, low profile cavity slot antenna will be investigated. Furthermore, array configuration of this antenna will be investigated and the system will be applied to the mobile satellite communications or the base station of the wireless LAN system.

References

[1] K. Fujimoto and J.R. James, Mobile Antenna Systems Handbook, Artech House, Boston, London, 1994.
[2] S. Ohmori, "Vehicle antennas for mobile satellite communications," IEICE Trans., vol.E74, no.10, pp.3210–3221, Oct. 1991.
[3] Engineering Test Satellite VIII (ETS-VIII) project, JAXA homepage http://www.jaxa.jp/missions/projects/sat/tsushin/ets8/index_e.html
[4] D.M. Pozar and S.M. Duffy, "A dual-band circularly polarized aperture-coupled stacked microstrip antenna for global positioning satellite," IEEE Trans. Antennas Propag., vol.45, no.11, pp.1618–1625, Nov. 1999.
[5] N.C. Karamakar and M.E. Bialkowski, "Circularly polarized aperture-coupled circular microstrip patch antennas for L-band applications," IEEE Trans. Antennas Propag., vol.47, no.5, pp.933–940, May 1999.
[6] W.S.T. Rowe and R.B. Waterhouse, "Investigation into the performance of proximity coupled stacked patches," IEEE Trans. Antennas Propag., vol.54, no.6, pp.1693–1698, June 2006.
[7] Y. Murakami, W. Chujo, I. Chiba, and M. Fujise, "Dual slot-coupled microstrip antenna for dual frequency operation," Electron. Lett., vol.29, no.22, pp.1906–1907, Oct. 1993.
[8] Y. Rikuta and H. Arai, "A self-diplexing antenna using slitted patch antenna," 2002 Interim International Symposium on Antennas and Propagation, pp.121–124, Nov. 2002.
[9] W. Chujo, M. Fujise, M. Nakano, H. Arai, and N. Goto, "A two-layer self-diplexing antenna using a circularly polarized ring patch antenna," IEICE Trans., vol.E74, no.10, pp.3261–3267, Oct. 1991.
[10] R. Garg, P. Bhartia, I. Bahl, and A. Ittipiboon, Microstrip Antenna Design Handbook, chap. 8, Artech House, Boston, London, 2001.
[11] G. Splitt and M. Davidovitz, "Guidelines for design of electromagnetically coupled microstrip patch antennas on two-layer substrates," IEEE Trans. Antennas Propag., vol.38, no.7, pp.1136–1140, July 1990.
[12] M. Yamamoto, K. Ishizaki, M. Muramoto, K. Sasaki, and K. Itoh, "Cavity-backed slot array antenna with backward excitation," IEICE Trans. Commun. (Japanese Edition), vol.J83-B, no.12, pp.1730–1738, Dec. 2000.
[13] T. Hirano, J. Hirokawa, and M. Ando, "Waveguide matching crossed-slot," IEE Proc. Microw. Antennas Propag., vol.150, no.3, pp.143–146, June 2003.
[14] K.C. Gupta, R. Garg, I. Bahl, and P. Bhartia, "T-Junction," in Microstrip lines and slotlines, pp.208–211, Artech House, Boston, 1996.
[15] J.P. Ki and W.S. Park, "Network modeling of an inclined and off-center microstrip-fed slot antenna," IEEE Trans. Antennas Propag., vol.46, no.8, pp.1182–1188, Aug. 1998.
[16] H. Iwasaki, "A circularly polarized rectangular microstrip antenna using single-fed proximity-coupled method," IEEE Trans. Antennas Propag., vol.43, no.8, pp.895–897, Aug. 1995.
[17] J.T.S. Sumantyo, K. Ito, D. Delaune, T. Tanaka, T. Onishi, and H. Yoshimura, "Numerical analysis of ground plane size effects on patch array antenna characteristics for mobile satellite communications," Int. J. Numer. Model., vol.18, no.2, pp.95–106, March/April 2005.
[18] V. Natarajan, E. Chettiar, and D. Chatterjee, "Effect of ground plane size on the performance of a class of microstrip antennas on microwave substrates," Proc. 2004 IEEE AP-S Int. Symp., vol.4, pp.4491–4494, June 2004.
[19] J. Huang, "The finite ground plane effect on the microstrip antenna radiation patterns," IEEE Trans. Antennas Propag., vol.31, no.4, pp.649–653, July 1983.
[20] B. Stockbroeckx, I. Huynen, and A.V. Vorst, "Effect of surface wave diffraction on radiation pattern of slot antenna etched in finite ground plane," IEE Electron. Lett., vol.36, no.17, pp.1444–1446, Aug. 2000.

Toshimitsu Tanaka was born in Chiba, Japan, on April 28, 1977. He received the B.S. and M.S. degrees from Chiba University, Chiba, Japan, in 2001 and 2004, respectively He is presently with the Graduate School of Science and Technology, Chiba University, Japan where he is working toward the Ph.D. degree. His main interest is the analysis and design of antennas and associated components for mobile satellite communications. He received an IEICE Young Researcher's Award in 2006. He is a student member of the IEEE. Since 2006 he has been employed as a Research Fellow of the Japan Society for the Promotion of Science.

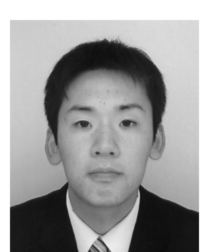

Tamotsu Houzen was born in Toyama, Japan, on December 7, 1983. He received the B.S. degree from Chiba University, Chiba, Japan, in 2006. He is presently with the Graduate School of Science and Technology, Chiba University, Japan where he is working toward the M.S. degree. His main interest is the analysis and design of antennas for mobile satellite communications and small antennas.

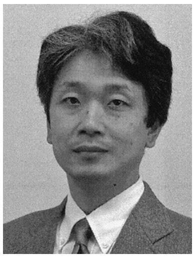

Masaharu Takahashi was born in Chiba, Japan, on December 15, 1965. He received the B.E. degree in electrical engineering in 1989 from Tohoku University, Miyagi, Japan, and the M.E. and D.E. degrees in electrical enginnering from the Tokyo Institute of Technology, Tokyo, Japan, in 1991 and 1994, respectively. He was a Research Associate from 1994 to 1996, an Assistant Professor from 1996 to 2000 with the Musashi Institute of Technology, Tokyo, Japan; and an Associate Professor from 2000 to 2004 with the Tokyo University of Agriculture and Technology, Tokyo, Japan. He is currently an Associate Professor with Chiba University, Chiba, Japan. His main interests include electrically small antennas, planar array antennas (RLSA), electromagnetic compatibility (EMC) and the research on the evaluation of the interaction between electromagnetic fields and the human body by use of numerical and experimental phantoms. He was the recipient of the 1994 IEEE Antennas and Propagation Society Tokyo Chapter Young Engineer Award. He is a senior member of the IEEE.

Koichi Ito was born in Nagoya, Japan, in June 1950. He received the B.S. and M.S. degrees from Chiba University, Chiba, Japan, in 1974 and 1976, respectively, and the D.E. degree from Tokyo Institute of Technology, Tokyo, Japan, in 1985, all in electrical engineering. From 1976 to 1979, he was a Research Associate at Tokyo Institute of Technology. From 1979 to 1989, he was a Research Associate at Chiba University. From 1989 to 1997, he was an Associate Professor at the Department of Electrical and Electronics Engineering, Chiba University, and is currently a Professor at the Research Center for Frontier Medical Engineering as well as at the Faculty of Engineering, Chiba University. In 1989, 1994, and 1998, he stayed at the University of Rennes I, France, as an Invited Professor. His main interests include analysis and design of printed antennas and small antennas for mobile communications, research on evaluation of the interaction between electromagnetic fields and the human body by use of numerical and experimental phantoms, and microwave antennas for medical applications such as cancer treatment. He is a Member of the AAAS, the Institute of Image Information and Television Engineers of Japan (ITE), the Japanese Society of Hyperthermic Oncology, and an IEEE Fellow. He served as Chair of Technical Group on Radio and Optical Transmissions of ITE from 1997 to 2001. He also served as Chair of the IEEE AP-S Japan Chapter from 2001 to 2002. He is now Chair of the Technical Group on Human Phantoms for Electromagnetics, IEICE, Vice-Chair of the 2007 International Symposium on Antennas and Propagation (ISAP2007), and an Associate Editor of the IEEE Transactions on Antennas and Propagation.